

University of Louisville

ThinkIR: The University of Louisville's Institutional Repository

Faculty Scholarship

11-1-2021

Galaxy And Mass Assembly (GAMA): The Merging Potential of Brightest Group Galaxies

K. Banks

S. Brough

Benne Holwerda

University of Louisville, benne.holwerda@louisville.edu

A. M. Hopkins

Á. R. López-Sánchez

See next page for additional authors

Follow this and additional works at: <https://ir.library.louisville.edu/faculty>



Part of the [Astrophysics and Astronomy Commons](#)

Original Publication Information

Banks, K., et al. "Galaxy And Mass Assembly (GAMA): The Merging Potential of Brightest Group Galaxies" 2021, *The Astrophysical Journal*, 921(1): 1-9.

ThinkIR Citation

Banks, K.; Brough, S.; Holwerda, Benne; Hopkins, A. M.; López-Sánchez, Á. R.; Phillipps, S.; Pimblet, K. A.; and Robotham, A. S. G., "Galaxy And Mass Assembly (GAMA): The Merging Potential of Brightest Group Galaxies" (2021). *Faculty Scholarship*. 826.

<https://ir.library.louisville.edu/faculty/826>

This Article is brought to you for free and open access by ThinkIR: The University of Louisville's Institutional Repository. It has been accepted for inclusion in Faculty Scholarship by an authorized administrator of ThinkIR: The University of Louisville's Institutional Repository. For more information, please contact thinkir@louisville.edu.

Authors

K. Banks, S. Brough, Benne Holwerda, A. M. Hopkins, Á. R. López-Sánchez, S. Phillipps, K. A. Pimblet, and A. S. G. Robotham



Galaxy And Mass Assembly (GAMA): The Merging Potential of Brightest Group Galaxies

K. Banks¹ , S. Brough¹ , B. W. Holwerda² , A. M. Hopkins³ , Á. R. López-Sánchez³ , S. Phillipps⁴,
K. A. Pimblet^{5,6} , and A. S. G. Robotham⁷

¹ School of Physics, University of New South Wales, NSW 2052, Australia

² Department of Physics and Astronomy, 102 Natural Science Building, University of Louisville, Louisville KY 40292, USA

³ Australian Astronomical Optics, Macquarie University, 105 Delhi Rd, North Ryde, NSW 2113, Australia

⁴ HH Wills Physics Laboratory, University of Bristol, Tyndall Avenue, Bristol, BS8 1TL, UK

⁵ School of Physics, Monash University, Clayton, Victoria 3800, Australia

⁶ E.A. Milne Centre for Astrophysics, University of Hull, Cottingham Road, Kingston-upon-Hull, HU6 7RX, UK

⁷ ICRAR, The University of Western Australia, 35 Stirling Highway, Crawley, WA 6009, Australia

Received 2021 May 2; revised 2021 July 13; accepted 2021 August 6; published 2021 October 29

Abstract

Using a volume-limited sample of 550 groups from the Galaxy And Mass Assembly Galaxy Group Catalogue spanning the halo mass range $12.8 < \log[M_h/M_\odot] < 14.2$, we investigate the merging potential of central Brightest Group Galaxies (BGGs). We use spectroscopically confirmed close-companion galaxies as an indication of the potential stellar mass buildup of low-redshift BGGs, $z \leq 0.2$. We identify 17 close-companion galaxies with projected separations $r_p < 30$ kpc, relative velocities $\Delta v \leq 300$ km s⁻¹, and stellar mass ratios $M_{\text{BGG}}/M_{\text{CC}} \leq 4$ relative to the BGG. These close-companion galaxies yield a total pair fraction of 0.03 ± 0.01 . Overall, we find that BGGs in our sample have the potential to grow in stellar mass due to mergers by $2.2 \pm 1.5\%$ Gyr⁻¹. This is lower than the stellar mass growth predicted by current galaxy evolution models.

Unified Astronomy Thesaurus concepts: [Galaxy evolution \(594\)](#); [Galaxy groups \(597\)](#); [Early-type galaxies \(429\)](#)

1. Introduction

Brightest Group Galaxies and Brightest Cluster Galaxies (BGGs and BCGs; e.g., Collins et al. 2009; Lidman et al. 2012; Oliva-Altamirano et al. 2014; Webb et al. 2015) are some of the most massive and most luminous galaxies observed in the universe. They are identified within massive galaxy groups and clusters, which are the largest gravitationally bound structures in the universe. BGGs and BCGs are often located at or near the center of groups and clusters and are predicted to be the final stage of galaxy evolution. Due to their characteristically high luminosity, they can be observed at large distances in the universe and are easily identified in cosmological simulations. These characteristics make them a particular focus of galaxy evolution studies.

BGGs and BCGs are predicted to increase in stellar mass in two phases. In the early stages of their evolution ($z \geq 2$), star formation dominates their stellar mass growth; however, once star formation is quenched, their stellar mass growth is predicted to be dominated by galaxy mergers at $z \leq 1$ (e.g., De Lucia & Blaizot 2007; Laporte et al. 2013; Contini et al. 2014; Webb et al. 2015; Gozaliasl et al. 2016; Cerulo et al. 2019; Cooke et al. 2019). It is evident from images that BCGs are often closely surrounded by other galaxies (e.g., Schombert 1987). These cluster members eventually spiral into the center of the cluster potential due to dynamical friction, ultimately merging with the BCG located at the center. Thus, the high mass of BCGs is attributed to their unique location near the center of galaxy clusters (e.g., Gunn et al. 1972). This mechanism is supported by observations (e.g., O’Dea et al. 2008, 2010; Zhao et al. 2017).

There is a strong observed relationship between a BCG’s stellar mass (M_*) and the mass of the dark matter halo it resides in (M_{halo} ; i.e., its host cluster environment). More massive central

galaxies are often associated with more massive haloes and the richness of their clusters/groups (i.e., the number density of galaxy members in a cluster/group; e.g., Liu et al. 2009; Zhao et al. 2015). The exact relationship has been examined in many studies (e.g., Lin & Mohr 2004; Popesso et al. 2007; Brough et al. 2008; Hansen et al. 2009; Lidman et al. 2012; Oliva-Altamirano et al. 2014; Lavoie et al. 2016; Kravtsov et al. 2018), which find the slope of $M_* - M_{\text{halo}}^b$ to be less than unity at $z < 1$. This implies that, while the BCG and cluster grow together, the halo gains mass (by merging with other clusters and groups) significantly faster than the BCG.

The stellar mass growth of these galaxies can be measured observationally in two different ways. The first method involves directly examining stellar masses of samples at different redshifts (e.g., Collins et al. 2009; Lidman et al. 2012; Oliva-Altamirano et al. 2014; Liu et al. 2015; Bellstedt et al. 2016). This is strongly dependent on the observed stellar mass–halo mass relationship. Lidman et al. (2012) found that the stellar mass of BCGs increased by a factor of 1.8 ± 0.3 from $z = 0.9$ to $z = 0.2$. Oliva-Altamirano et al. (2014) compared a sample of 883 galaxies divided into higher ($0.17 \leq z \leq 0.27$) and lower redshift bins ($0.09 \leq z \leq 0.17$) from the Galaxy And Mass Assembly Survey (GAMA; Driver et al. 2011). They found no significant growth in the stellar mass of BGGs or BCGs over ~ 2 Gyr from $z = 0.27$ to $z = 0.09$.

The second method predicts the stellar mass growth of these galaxies by examining the mass in close-companion galaxies available to merge with the central galaxy within a few gigayears (e.g., McIntosh et al. 2008; Liu et al. 2009; Groenewald et al. 2017).

Observational studies to date of the stellar mass growth of central galaxies due to mergers have used samples that are either spectroscopically incomplete or use photometric

redshifts (e.g., McIntosh et al. 2008; Liu et al. 2009, 2015; Groenewald et al. 2017). These studies will likely suffer from incompleteness or from line-of-sight contamination. Some studies (e.g., Groenewald et al. 2017) use simulations to estimate a correction factor for the line-of-sight contamination. Others (e.g., McIntosh et al. 2008; Liu et al. 2009, 2015) identify close-companion galaxies based not only on their projected separation from the central galaxy, but also on the presence of morphological disturbances in those galaxies. These corrections, however, can increase the uncertainties in these measurements.

The observations of the stellar mass buildup of central galaxies agree with simulations at high redshifts ($z > 0.5$), but there is a large discrepancy between simulations and observations at lower redshifts (e.g., $z \leq 0.5$; Laporte et al. 2013; Lidman et al. 2013; Lin et al. 2013; Contini et al. 2014). For example, both De Lucia & Blaizot (2007) and Laporte et al. (2013) find that BGGs grow by a factor of ~ 1.8 at $z < 0.5$. This corresponds to an average fractional stellar mass growth of $\sim 15\%$ per gigayear, whereas observational studies such as McIntosh et al. (2008); Liu et al. (2009, 2015); Oliva-Altamirano et al. (2014) find significantly less growth.

In this paper, we investigate the potential stellar mass growth of central BGGs between $0.07 \leq z \leq 0.20$ by analyzing a volume-limited sample of groups selected from the Galaxy And Mass Assembly survey (GAMA; Driver et al. 2011). GAMA offers a very large sample of galaxy groups that cover a wide range of total halo masses ($10^{10.3} - 10^{15.0} M_\odot$). GAMA’s high spectroscopic completeness (98.5%; Liske et al. 2015) allows us to robustly examine the influence of merging close-companion galaxies on the stellar mass buildup of BGGs.

In Section 2, we outline the data source for this paper, the GAMA survey (Driver et al. 2011), and the different catalogs used within our analysis. Section 3 details the selection of our volume-limited sample and describes the methods used to ensure a robust analysis. In Section 4, we describe the steps of our method and the calculations that allow us to investigate the stellar mass growth of BGGs in our sample. A discussion of our results and their comparison to other similar observational studies as well as semianalytical models is presented in Section 5. Finally, we summarize our conclusions in Section 6. Throughout this paper, we assume a flat Λ CDM cosmology with $h = 0.7$, $H_0 = 100h \text{ km s}^{-1} \text{ Mpc}^{-1}$, $\Omega_m = 0.3$, and $\Omega_\Lambda = 0.7$.

2. The Galaxy And Mass Assembly (GAMA) Survey

The Galaxy And Mass Assembly (GAMA) survey is a wide-field, multiwavelength galaxy redshift survey that probes the local universe ($z \leq 0.5$; Driver et al. 2011). Spectroscopic observations were taken with the 3.9 m Anglo-Australian Telescope in conjunction with the AAOmega multiobject spectrograph. The spectroscopic observations are highly complete, with 98.5% of galaxies having a robust distance measurement (Hopkins et al. 2013; Liske et al. 2015). GAMA also has a particular focus on high pair fraction completeness that is crucial for this analysis. This level of completeness was achieved by returning to observe each target area an average of 10 times (Robotham et al. 2010).

The GAMA survey consists of $\sim 300,000$ galaxies with a magnitude limit of $r < 19.8 \text{ mag}$ over $\sim 286 \text{ deg}^2$ across five regions of the sky. This study analyzes the galaxies within the three main survey regions, G09, G12, and G15, known as the

equatorial regions (Driver et al. 2011). Survey data is made available in Data Management Units (DMUs) that collate measurements from different analyses. The group-finding and stellar mass DMUs are of particular use to this analysis and are described in the following sections.

2.1. The GAMA Galaxy Group Catalogue (G^3C)

The GAMA Galaxy Group Catalogue (G^3C) is the catalog of all of the galaxy groups defined in the GAMA survey (Robotham et al. 2011). We use version 10 of the catalog here and briefly describe the key measurements.

The G^3C uses a friends-of-friends (FoF) algorithm to identify groups. The halo mass is estimated using the measured values of the halo velocity dispersion (σ) and the group radius (R). The halo velocity dispersion is calculated using the *gapper* estimator introduced by Beers et al. (1990), which is developed to be robust to outliers in smaller number samples. The group radius used is that which contains 50% of galaxies in the group (R_{50}). This is chosen such that the group radius is robust against potential interloping galaxies (Robotham et al. 2011). For a stable system, the halo mass equates to $M_{\text{halo}} = A\sigma^2 R$. In GAMA, the constant A is calculated by comparison between the group-finder outputs from observations and mock observations of simulations (Robotham et al. 2011), and the total halo mass of a group is estimated as $M = 10.0\sigma^2 R$. We also estimated the impact of determining halo masses of our groups using the weak-lensing-calibrated halo mass scaling relations in Viola et al. (2015) and find that these do not qualitatively change our conclusions.

Three approaches were considered to determine the central galaxy of GAMA groups in Robotham et al. (2011). The first approach determined the center of the cluster to be the center of light, which is a good proxy for center of mass. The second approach was an iterative process where the center of light was derived at each step from the r_{AB} -band luminosity of all the galaxies identified within the group. The most distant galaxy from the center of light was rejected. This process was repeated until two galaxies remained, of which the brighter r_{AB} -band galaxy was used as the group center. The third approach simply defined the group center by the brightest member of the group, i.e., the BGG. Robotham et al. (2011) found that the iterative method produced the most robust estimate of the central galaxy of the group, and we therefore use that here.

2.2. GAMA Stellar Mass Catalog

The stellar masses of galaxies in the GAMA survey are estimated by Taylor et al. (2011) by fitting model spectral energy distributions to Sloan Digital Sky Survey (SDSS; York et al. 2000) *ugriz* imaging reprocessed by the GAMA team (Hill et al. 2011). When observing galaxies at varying distances with an aperture of a fixed size, different fractions of a galaxy’s luminosity will be observed. The flux of each galaxy is measured within a flexible circular aperture, where the size of the aperture is determined by the observed radial surface brightness profile of the galaxy. Since only a fraction of each galaxy’s luminosity is considered for the stellar mass estimate, a linear scale factor, *fluxscale*, is calculated to account for the unobserved luminosity of each galaxy from the ratio between the aperture r -band flux and the total r -band flux inferred from fitting a single Sérsic profile truncated at $10 R_e$ (Kelvin et al. 2012). We apply this scale factor in this work.

3. Sample Selection

The G³C equatorial regions contain 23,654 groups with 75,029 constituent members. Estimated parameters for groups within the G³C, such as the projected radius Rad_{50} , velocity dispersion σ , and halo mass M_{halo} , are robust for groups that contain five or more galaxy members ($N_{\text{FoF}}; \text{Robotham et al. 2011}$). Hence, we only include groups with five or more galaxy members in our analysis, $N_{\text{FoF}} \geq 5$. This reduces our sample to 2754 groups. Furthermore, five groups with $N_{\text{FoF}} \geq 5$ have an estimated velocity dispersion $\sigma = 0$, since the error in the raw velocity distribution σ_{err} is larger than the raw velocity distribution σ_{gap} . Hence, we do not include these five groups in this analysis.

In this study, we wish to examine groups where the identified BGG is at the center of the group; therefore, we choose groups in our sample where the BGG is also identified as the iterative central galaxy. Selecting groups where the BGG is also identified as the iterative central gives us a sample of 2,363 groups.

There are two BGGs within the G³C that do not have a measured stellar mass within the Stellar Mass catalog, likely due to contamination in one of the images. We exclude the groups that host these two BGGs from our sample. This leaves us with a sample of 2361 groups.

3.1. BGG Selection

The GAMA survey is apparent magnitude limited; we therefore select a volume-limited sample to ensure a robust analysis.

The distribution of BGG stellar mass with redshift is shown in the top panel of Figure 1. The density of BGGs with $z \sim 0.25$ is lower compared to the rest of the sample, due to the 5577 Å sky line passing through key spectral features. We therefore limit our sample to groups with redshifts $z < 0.2$. We also impose a lower limit on the redshift, $z \geq 0.07$, due to the low volume sampled below this.

We define a minimum BGG stellar mass limit across our sample such that this minimum stellar mass is observed for galaxies of all colors across our redshift range. At $z = 0.2$, this minimum complete BGG stellar mass is $10^{11.0} M_{\odot}$, which we apply to our sample. We also apply an upper limit, $10^{11.6} M_{\odot}$, on the stellar mass of BGGs to remove unrealistically massive BGGs that likely occur as a result of image contamination. This volume limit yields a sample of 640 groups. The distribution of halo mass is also affected by GAMA's apparent magnitude selection limit. We apply a volume limit to this too, limiting the halo mass of groups to a lower limit of $M_h = 10^{12.8} M_{\odot}$ and an upper limit of $10^{14.2} M_{\odot}$. This selection results in a volume-limited sample of 550 groups and is illustrated in Figure 1 with BGG stellar mass in the top panel and group halo mass in the bottom panel.

3.2. Close-companion Galaxy Selection

Our sample of 550 groups contains 4207 noncentral member galaxies that have the potential to merge with their BGG (illustrated by the gray points in Figure 2). The distribution of these galaxies in redshift is similarly affected by GAMA's apparent magnitude selection limit. We place a conservative initial volume limit of $M^* = 10^{10.2} M_{\odot}$ allowing for the range of galaxy colors at GAMA's $m_r = 19.8$ mag limit at our $z \sim 0.2$ limit. This yields a maximum possible BGG-to-companion

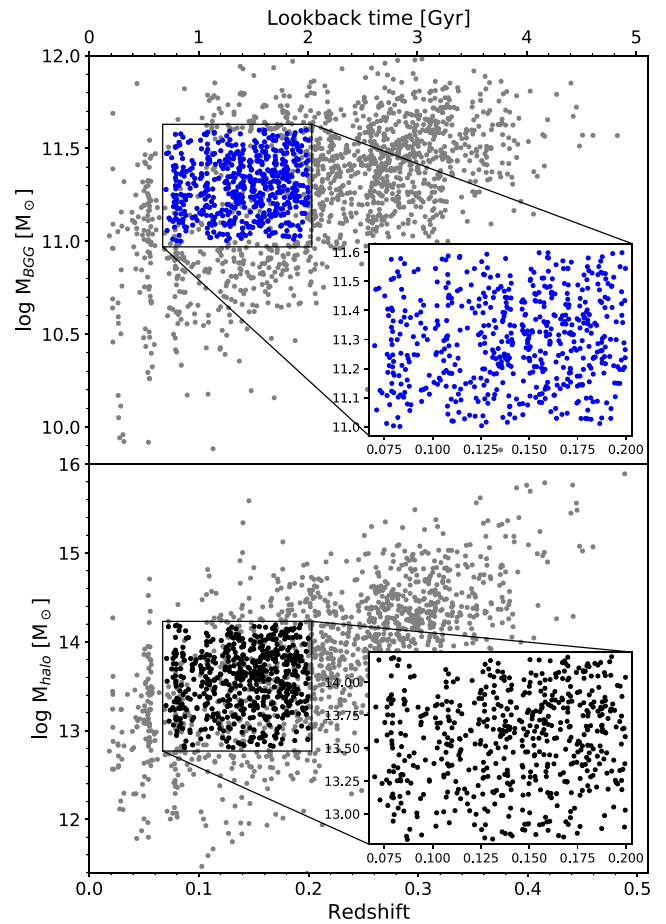


Figure 1. Selection of BGG sample as a function of stellar mass and redshift (top panel). Selection of BGG sample as a function of halo mass and redshift (bottom panel). The gray points represent the preliminary G³C sample without BCG/halo mass selection; the blue points in the top panel and the black points in the bottom panel illustrate the final group sample selection with respect to BCG stellar mass and halo mass, respectively.

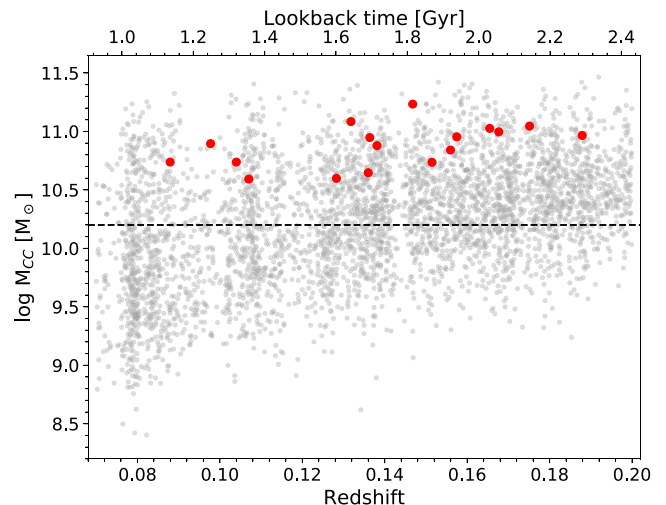


Figure 2. Selection of close-companion galaxies illustrated with respect to redshift and companion galaxy stellar mass. The gray points represent the noncentral galaxy members of groups in our sample, and the red points illustrate the close-companion galaxies identified from our selection criteria. The dotted black line at $\log M_{\text{CC}} = 10.2 M_{\odot}$ illustrates the lower stellar mass limit of our sample of close-companion galaxies.

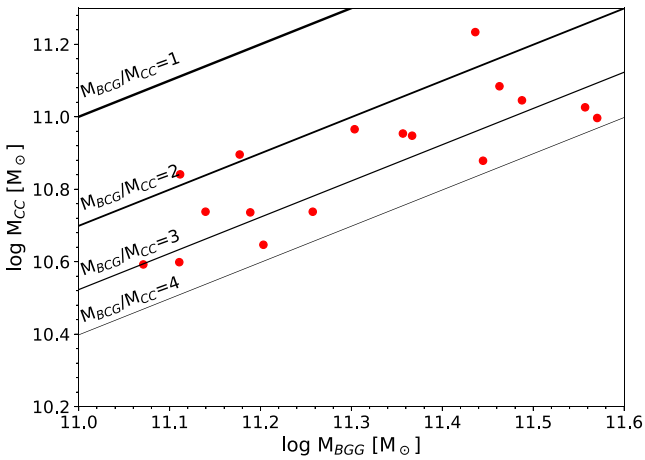


Figure 3. Distribution of close-companion galaxies within our sample with respect to BGG stellar mass. Each black line represents a BGG-to-CC mass ratio equipotential, with the thickest line representing a mass ratio equivalent to 1 and the weakest line equivalent to 4. This illustrates that the companions in our sample are spread uniformly across stellar mass ratios.

stellar mass ratio $M_{\text{BGG}}/M_{\text{CC}} \sim 6$ when compared to the least massive BGGs in our sample (i.e., $\sim 10^{11.0} M_{\odot}$).

Within the literature (e.g., De Lucia & Blaizot 2007; McIntosh et al. 2008; Liu et al. 2009; Robotham et al. 2014; Groenewald et al. 2017), a close-companion galaxy with a BGG-to-companion stellar mass ratio $M_{\text{BGG}}/M_{\text{CC}} \leq 4$ is considered a major merger, whereas those with stellar mass ratios > 4 are considered minor mergers. The lower stellar mass limit imposed on our sample of potential close-companion galaxies does not produce a robust sample of minor merger candidates. Henceforth, we focus only on major mergers with stellar mass ratios $M_{\text{BGG}}/M_{\text{CC}} \leq 4$.

A galaxy may be considered a close companion to a BGG if it has a small projected separation (r_p) and relative velocity (Δv) to the BGG. Taking into account both of these parameters ensures an unbiased sample with less of the line-of-sight contamination that may be present in purely photometric samples (Kitzbichler & White 2008).

A recent analysis of the ILLUSTRIS-1 simulation (Vogelsberger et al. 2014; Ventou et al. 2019) suggests that major close-companion galaxies at low redshift ($z < 0.5$) with a projected distance $r_p \leq 25$ kpc and a velocity of $\Delta v \leq 150$ km s $^{-1}$ relative to the BGG with stellar mass $> 10^{9.5} M_{\odot}$ have a 75% chance of merging by $z = 0$. Ventou et al. (2019) suggest the following selection criteria for selecting spectroscopic close-companion galaxies that are likely to merge: $r_p \leq 50$ kpc and $\Delta v \leq 300$ km s $^{-1}$. However, numerous observational studies (e.g., McIntosh et al. 2008; Liu et al. 2009; Robotham et al. 2014; Groenewald et al. 2017) apply a more conservative projected separation of $r_p \leq 30$ kpc.

To construct a robust sample of close-companion galaxies, we follow the recommendations of Ventou et al. (2019) and identify close-companion galaxies as galaxies with $\Delta v \leq 300$ km s $^{-1}$ and use the conservative projected separation limit $r_p \leq 30$ kpc. This selection criteria results in 17 close-companion galaxies. We note here that when we expand the sample to $r_p \leq 50$ kpc, the sample increases to 31 close-companion galaxies. To be consistent with the literature, we only consider those within $r_p \leq 30$ kpc for the remainder of our analysis. These close-companion galaxies are represented by the red points in Figure 2.

Figure 3 illustrates the distribution of companion stellar mass with respect to BGG stellar mass and demonstrates equivalent BGG-to-CC stellar mass ratios. Each black line represents stellar mass ratios with the thickest line representing $M_{\text{BGG}}/M_{\text{CC}} = 1$ and the weakest line equivalent to 4. This illustrates that the companions within our sample are distributed uniformly between stellar mass ratios $1 \leq M_{\text{BGG}}/M_{\text{CC}} < 4$.

4. Stellar Mass Growth of BGGs

We are analyzing the potential for stellar mass growth of BGGs over the redshift range $0.07 \leq z \leq 0.20$. We also investigate whether there is any dependence on the halo mass of their host cluster, which we use as a tracer of the environment of the BGGs.

4.1. Pair Fraction

We investigate the fraction of close-companion galaxies within our sample. This is also known as the pair fraction and is defined as:

$$f_{\text{pair}} = \frac{N_{\text{CCs}}}{N_{\text{BGGs}}}, \quad (1)$$

where N_{BGGs} is the total number of BGGs in the sample and N_{CCs} is the total number of identified close-companion galaxies. The 1σ uncertainties used throughout are calculated using the binomial confidence interval described in Cameron (2011), because it is robust to the small sample sizes present in our analysis.

Given that we have a sample of 550 BGGs and identified 17 close-companion galaxies within our sample of noncentral galaxies, this yields a pair fraction of $f_{\text{pair}} = 0.03 \pm 0.01$. However, as mentioned in Section 3.2, simulations show that close-companion galaxies with $r_p \leq 25$ kpc and $\Delta v \leq 150$ km s $^{-1}$ have a 75% chance of merging by $z = 0$ so the pair fraction calculated here is an upper limit. The pair fraction is henceforth used to calculate the maximum potential stellar mass growth of the BGGs in our sample.

We also investigate the influence of halo mass on the BGG pair fraction and illustrate this in Figure 4. While there is no statistically significant dependence in this halo mass range (i.e., $10^{12.8} M_{\odot} \leq M_{\text{halo}} \leq 10^{14.2} M_{\odot}$), we do note a systematic decrease of the BGG pair fraction with increasing halo mass. We also investigated this relationship with the less conservative limit of $r_p \leq 50$ kpc and found a similar result.

4.2. Merger Rate

The next step in determining the potential stellar mass growth of BGGs is to calculate their merger rate, which requires knowledge of the time it takes for a close-companion galaxy to merge with the BGG, i.e., the merging timescale. A commonly used merging timescale in galaxy merging literature is that derived by Kitzbichler & White (2008) using the Millenium Simulation (Springel et al. 2005).

Kitzbichler & White (2008) find that at redshifts $z \ll 1$, the average merging timescale derived for a close-companion galaxy with stellar mass $> 5 \times 10^9 h^{-1} M_{\odot}$, within $\Delta v \leq 300$

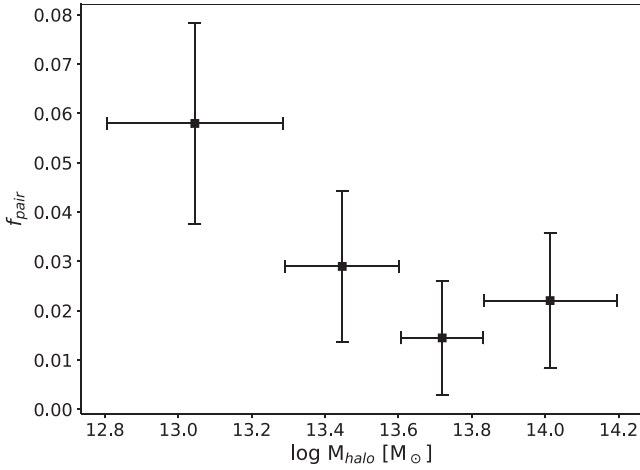


Figure 4. BGG pair fraction as a function of halo mass. We find no statistically significant dependence of the BGG pair fraction on halo mass over our halo mass range $10^{12.8} M_{\odot} \leq M_{\text{halo}} \leq 10^{14.2} M_{\odot}$. We do note, however, a systematic decrease of the BGG pair fraction with increasing halo mass. This is also present with a less conservative limit of $r_p \leq 50$ kpc on the close-companion galaxies.

km s^{-1} and a projected radius $r_p \leq 50$ kpc, is given by:

$$\langle T_{\text{merge}} \rangle = T_0 \frac{r_p}{r_0} \left(\frac{M_*}{M_0} \right)^{-0.3} \left(1 + \frac{z}{8} \right), \quad (2)$$

where $T_0 = 2.2$ Gyr, $r_0 = 50 h^{-1}$ kpc, $M_0 = 4 \times 10^{10} h^{-1} M_{\odot}$, and z is the median redshift of the cluster. Using this method, the close-companion galaxies identified in this work are predicted to merge with their respective BGGs in 0.53 ± 0.19 Gyr on average.

Other recent investigations into the average merger rate of galaxies use an observability timescale (e.g., Lotz et al. 2008, 2011; Mundy et al. 2017; Duncan et al. 2019). This observability timescale is the average timescale during which merging galaxies can be observed depending on the method used to identify the merger (e.g., close galaxy pair selection utilized in this work). Lotz et al. (2011) derive this quantity for a number of merger selections. They suggest that the timescale for major close-companion galaxies identified through pair selection is ~ 0.33 Gyr for $5 h^{-1} < r_p < 20 h^{-1}$ kpc, and ~ 0.63 Gyr for $10 h^{-1} < r_p < 30 h^{-1}$ kpc, which is consistent with the merging timescale calculated for our close-companion galaxies using Equation (2). In order to provide a robust comparison to previous analyses (e.g., McIntosh et al. 2008; Liu et al. 2009; Groenewald et al. 2017) of the stellar mass growth of BGGs we use the timescales predicted by Kitzbichler & White (2008), which are also utilized in these previous studies.

The average merger rate of a sample of BGGs, i.e., the number of mergers per BGG per gigayear is then calculated as follows:

$$\langle R_{\text{merge}} \rangle = \frac{f_{\text{pair}}}{\langle T_{\text{merge}} \rangle}. \quad (3)$$

The uncertainty on $\langle R_{\text{merge}} \rangle$ is calculated using the standard propagation of uncertainties.

The close-companion galaxies in our sample of groups merge with their respective BGGs in 0.53 ± 0.19 Gyr on

average. Therefore, the BGGs in our sample experience on average 0.06 ± 0.03 mergers per gigayear.

4.3. Average Stellar Mass Growth

The potential stellar mass growth rate of BGGs, ΔM_* ($M_{\odot} \text{Gyr}^{-1}$) is calculated using a modified version of Equation (7) from Groenewald et al. (2017). Their equation determines the overall growth of BGGs evolved from a particular redshift to $z = 0$. In this study we are interested in the potential average mass growth of BGGs at low redshifts, so we modify their equation such that the result is the average stellar mass growth per gigayear. Our modified equation is as follows:

$$\Delta M_* = \langle R_{\text{merge}} \rangle \times \langle M_* \rangle_{\text{CC}}, \quad (4)$$

where $\langle M_* \rangle_{\text{CC}}$ is the average stellar mass of the close-companion galaxies in our sample in M_{\odot} .

The close-companion galaxies in our sample have an average stellar mass of $\langle M_* \rangle_{\text{CC}} = 8.18 \pm 3.34 \times 10^{10} M_{\odot}$, which contribute a total stellar mass of $\Delta M_* = 0.47 \pm 0.30 \times 10^{10} M_{\odot}$ per gigayear.

4.4. Fractional Stellar Mass Growth

We calculate the fractional contribution of mergers toward the stellar mass growth of BGGs per gigayear. We modify Equation (8) from Groenewald et al. (2017) to calculate the fractional contribution made by merging close-companion galaxies in our sample but not incorporating their growth to $z = 0$. This is defined per gigayear, by:

$$F = \frac{\Delta M_*}{\langle M_* \rangle_{\text{BGG}}(t=0) + \Delta M_*}, \quad (5)$$

where $\langle M_* \rangle_{\text{BGG}}(t=0)$ is the average stellar mass of BGGs in the sample at the present day. While BGGs do grow in stellar mass from the formation of stars, it is rare to find star-forming BGGs at $z \leq 0.5$ ($< 1\%$; e.g., Liu et al. 2012; Fraser-McKelvie et al. 2014; Webb et al. 2015; Groenewald et al. 2017; Cerulo et al. 2019). Those BGGs that are forming stars grow by $\sim 1\%$ – 3% in stellar mass from star formation (e.g., Liu et al. 2012). Furthermore, it is estimated that the contribution of stellar mass to BGGs via minor mergers is just as significant as that through major mergers (e.g., Edwards & Patton 2012); however, we cannot robustly measure the stellar mass growth of BGGs due to minor mergers and so we focus here on their growth only via major mergers.

We find that BGGs in our sample spanning the redshift range $0.07 \leq z \leq 0.20$ grow in stellar mass due to major mergers by $2.19\% \pm 1.52\% \text{Gyr}^{-1}$, assuming that all of the stellar mass of a merging close-companion galaxy is accreted onto the BGG. This is similar to the predicted stellar mass growth from star formation of star-forming BGG ($\sim 1\%$ – 3% e.g., Liu et al. 2012)

5. Discussion

We have presented here an analysis of the potential stellar mass growth of BGGs in the GAMA survey from close-companion galaxies. In this section we compare our results (see Table 1) to the literature.

Table 1
Results.

Redshift	$\langle M_{\text{BGG}} \rangle$ [$10^{10} M_{\odot}$]	$\langle M_{\text{CC}} \rangle$ [$10^{10} M_{\odot}$]	f_{pair}	$\langle T_{\text{merge}} \rangle$ [Gyr]	$\langle R_{\text{merge}} \rangle$ [Gyr^{-1}]	ΔM_* [$10^{10} M_{\odot} \text{ Gyr}^{-1}$]	F [% Gyr^{-1}]
$0.07 \leq z \leq 0.2$	21.17 ± 7.48	8.18 ± 3.34	0.03 ± 0.01	0.53 ± 0.19	0.06 ± 0.03	0.47 ± 0.30	2.19 ± 1.52

Note. Column 1 is the redshift range of our sample. Columns 2 and 3 indicate the average stellar mass of the BGGs and close-companion galaxy (CCs) galaxies in our sample, respectively. Columns 4, 5, and 6 illustrate the pair fraction, average merging timescale, and average merger rate for the BGGs in our sample, respectively. Finally, columns 7 and 8 are the stellar mass growth of BGGs in our sample in solar masses per gigayear and fractional stellar mass growth per gigayear, respectively.

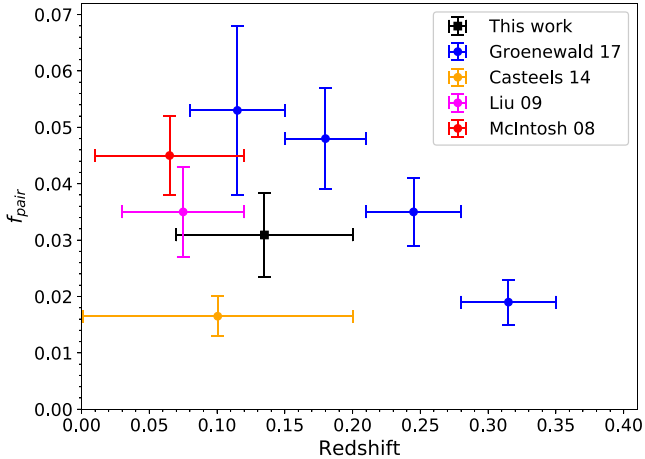


Figure 5. Major merger pair fraction considering close-companion galaxies within 30 kpc and with mass ratios ≤ 4 . Our result is presented as the black point. Other published pair fractions are plotted at the mean redshift of each sample while the horizontal error bars indicate the redshift range of the sample. The BGG pair fraction we calculate in our sample agrees well with previous results.

5.1. BGG Pair Fraction

In Figure 5 we compare our pair fraction to earlier studies. Both McIntosh et al. (2008) and Liu et al. (2009) have studied the BGG pair fraction at $z \leq 0.12$. McIntosh et al. (2008) investigated the incidence of major mergers with mass ratios ≤ 4 in the Sloan Digital Sky Survey (SDSS). They used a volume-limited sample of 845 groups with halo masses $> 2.5 \times 10^{13} M_{\odot}$ and refined their search for merger candidates within 30 kpc by visually inspecting their sample of 221 galaxy pairs for the presence of morphological features associated with merging events. This was done in lieu of setting a limit on the relative velocities of the close-companion galaxies due to the purely photometric sample used in their analyses. From this they found a pair fraction of $f_{\text{pair}} = 0.045 \pm 0.007$. This is represented by the red point in Figure 5.

Liu et al. (2009) similarly searched for ongoing major mergers (≤ 4) in a sample of BGGs from the SDSS C4 cluster catalog (Miller et al. 2005) with redshifts $0.03 \leq z \leq 0.12$. They also searched for close-companion galaxies within 30 kpc that showed significant signs of interaction in the form of significant asymmetry in residual images. They concluded that 18 of their 515 BGGs were involved in major mergers, i.e., $f_{\text{pair}} = 0.035 \pm 0.008$ indicated in Figure 5 by the magenta point.

The blue points in Figure 5 represent the pair fraction calculated in Groenewald et al. (2017). They studied more massive groups ($M_h > 2.2 \times 10^{15} M_{\odot}$) constructed from the redMaPPer catalog (Rykoff et al. 2014). They split their sample

into four redshift ranges, the first two of which overlap with the redshift covered by our sample. These two low redshift ranges result in a pair fraction $f_{\text{pair}} \sim 0.05$.

We calculate a major merger pair fraction of $f_{\text{pair}} = 0.03 \pm 0.01$ over similar redshifts to those in McIntosh et al. (2008), Liu et al. (2009) and Groenewald et al. (2017). This is in agreement with these earlier studies.

Casteels et al. (2014) also investigated the major merger pair fraction in the GAMA survey at redshifts $0.001 < z < 0.2$. They examined the mass-dependent major merger rate of GAMA galaxies with stellar masses $10^{8.0} < M_* < 10^{11.5} M_{\odot}$ and found the major merger pair fraction to be consistent at ~ 0.013 – 0.02 between $10^{9.5} < M_* < 10^{11.5} M_{\odot}$ an major merger pair fraction is approximately half the major merger pair fraction calculated in this work (i.e., 0.03 ± 0.01); however, we note that their sample is not limited to central galaxies, and so we do not directly compare it to our result in Figure 5.

We also investigate the role the BGG’s environment plays on the pair fraction (see Figure 4). Liu et al. (2009) also examined the relation between the fraction of BGGs involved in major mergers and the richness of the cluster, defined as the number of cluster members within a $1 h^{-1}$ Mpc radius centered on the BGG. The pair fraction of BGGs in Liu et al. (2009) appeared to increase with increasing cluster richness with a BGG pair fraction of ~ 0.01 at a richness of ~ 15 up to ~ 0.055 at a richness of ~ 45 . While our total pair fractions across halo mass are in agreement with those in Liu et al. (2009), Figure 4 shows that we find that the major merger pair fraction tends to decrease with halo mass, however, we note that relationship is not statistically significant.

5.2. Merger Rate

The BGG pair fraction and the mean merging timescale of close-companion galaxies are key ingredients in the calculation of the BGG merger rate. We have estimated the merging timescale of close-companion galaxies in our sample using the merging timescale derived in Kitzbichler & White (2008). The merging timescale is largely influenced by the stellar mass of the infalling close-companion galaxies and their projected separation from the BGG. Our sample of close-companion galaxies range in stellar mass between $10.5 < \log[M_*/M_{\odot}] < 11.2$ and have projected separations within 30 kpc. The mean merging timescale for all of the close-companion galaxies in our sample is 0.53 ± 0.19 Gyr.

A pair fraction of 0.03 ± 0.01 and a mean merging timescale of 0.53 ± 0.19 Gyr yields an average merger rate of $0.06 \pm 0.03 \text{ Gyr}^{-1}$. This implies that the BGGs in our sample experience on average one major merger every 16 Gyr since $z = 0.2$, significantly longer than the age of the universe. This is consistent with simulations (e.g., Hopkins et al. 2010) and

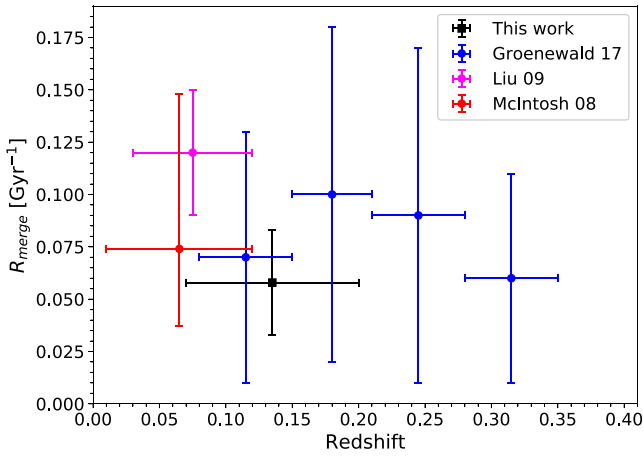


Figure 6. Comparison of the BGG major merger rate. Our result is presented by the black point. Other published merger rates are plotted at the mean redshift of each sample, while the horizontal error bars indicate the redshift range of the sample. Our result is consistent with previous studies; that is, BGGs do not experience significant numbers of major mergers per gigayear.

observations at similar redshifts (e.g., McIntosh et al. 2008; Edwards & Patton 2012; Liu et al. 2012).

Figure 6 shows the comparison of our measured merger rates with the previous studies introduced in Section 5.1. While some of these samples have higher stellar mass companions than our sample, we find them all to have consistent merger rates.

5.3. Stellar Mass Growth Rate of BGGs

The average merger rate and the mean stellar mass of close-companion galaxies are used to estimate the potential stellar mass growth rate of BGGs in our sample. The average stellar mass of the close-companion galaxies in our sample is $8.18 \pm 3.34 \times 10^{10} M_{\odot}$. The BGGs in our sample therefore increase their stellar mass by $0.47 \pm 0.30 \times 10^{10} M_{\odot} \text{ Gyr}^{-1}$ due to major mergers, which is equivalent to a fractional mass increase of $2.19 \pm 1.52\% \text{ Gyr}^{-1}$.

5.3.1. Observational Studies of Close-companion Galaxies

We compare the values calculated in McIntosh et al. (2008); Liu et al. (2009, 2015); Groenewald et al. (2017) with the stellar mass growth we have estimated in Figure 7. It is important to note that only McIntosh et al. (2008) have calculated the stellar mass growth of BGGs per gigayear. All other studies mentioned in this comparison estimate the stellar mass growth over a redshift range. In order to obtain a comparison to these results, we convert them to a stellar mass growth per gigayear by dividing the stellar mass growth by the lookback time that corresponds to the redshift range using the same cosmology.

Numerical simulations that investigate the buildup of the intracluster light (ICL; e.g., Conroy et al. 2007; Murante et al. 2007; Puchwein et al. 2010; Laporte et al. 2013; Contini et al. 2014) due to galaxy mergers predict that 30%–80% of a merging close-companion galaxy’s stellar mass contributes to the mass of the ICL rather than the BGG. Many observational studies that investigate the stellar mass buildup of BGGs take this into account and assume a conservative fraction, $f=0.5$ (e.g., Liu et al. 2009, 2015; Groenewald et al. 2017). This study investigates the potential for stellar mass buildup of BGGs,

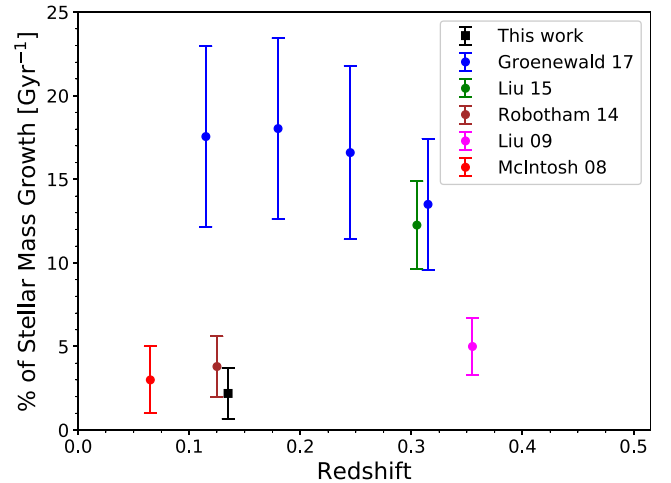


Figure 7. Comparison of the fractional stellar mass growth of BGGs per gigayear due to major mergers with respect to redshift. Our result is presented by the black point. Other published fractional stellar mass growth of BGGs are plotted at the average redshift of each sample. Overall, BGGs in our sample, as well as those from other samples, do not undergo a significant growth rate.

hence we do not assume this mass fraction. Henceforth, we divide out the fractions used in these studies to present a consistent comparison to our result.

McIntosh et al. (2008) estimate the rate of stellar mass accretion by major mergers via,

$$\dot{M}_{\text{BGG}} = \frac{\sum M_{*,i} f}{N_{\text{BGG}}} \times \frac{1}{t_{\text{merge}}}, \quad (6)$$

where N_{BGG} is the total number of BGGs in the sample; $M_{*,i}$ is the stellar mass of the i th close-companion galaxy; and f is the fraction of stellar mass of the companion galaxy that is accreted onto the BGG. They find that BGGs in large groups with redshifts $z \leq 0.12$ gain up to $2.4^{+1.1}_{-0.6} \times 10^{10} M_{\odot} \text{ Gyr}^{-1}$ assuming that all of the companion’s stellar mass is accreted onto the BGG. The stellar mass growth calculated by McIntosh et al. (2008) is equivalent to an average stellar mass growth of 1%–5% Gyr^{-1} . This is represented in Figure 7 by the red point.

Liu et al. (2009) found that major mergers contribute $5.0\% \pm 1.7\% \text{ Gyr}^{-1}$ when all of the major companion’s stellar mass is accreted onto the BGG. This is represented by the magenta point in Figure 7. In a later study, Liu et al. (2015) found that major mergers contribute 70% \pm 15% to the stellar mass of present day BGGs since $z = 0.6$. This corresponds to an average stellar mass growth of $12.2\% \pm 2.6\% \text{ Gyr}^{-1}$ from $z = 0.6$ (green point in Figure 7), which is substantially larger than their earlier estimate of the potential stellar mass growth rate as well as what we calculate here. We will return to this discrepancy later in this section.

Edwards & Patton (2012) also identify close-companion galaxies of BGGs in order to quantify the rate at which these galaxies grow via mergers. They used deep images from the Canada–France–Hawaii Telescope Legacy Survey and analyzed close-companion galaxies within 50 kpc (using photometric redshifts) of their BGGs with luminosity ratios up to $L_{\text{BGG}}/L_{\text{CC}} = 20$. The luminosity in major companions is $1.14 \pm 0.28 \times 10^{10} L_{\odot}$, whereas it is almost double when including minor companions, i.e., $2.14 \pm 0.31 \times 10^{10} L_{\odot}$. They find that these close-companion galaxies could increase the stellar mass of a $5 \times 10^{11} M_{\odot}$ BGG by up to $\sim 10\%$ over the

redshift range $0.15 \leq z \leq 0.39$. This potential stellar mass growth is attributed to both major and minor close-companion galaxies; therefore, we do not directly compare it to our result in Figure 7.

The stellar mass growth of galaxies from an earlier release of the GAMA Galaxy Group catalog was also investigated by Robotham et al. (2014). They investigated major mergers of galaxies with stellar masses $10^8 - 10^{12} M_{\odot}$ and found that the fraction of mass being added by merging is approximately 2.0%–5.6%. This is represented in Figure 7 by the dark red point.

Groenewald et al. (2017) investigated the stellar mass buildup of BGGs between $0.08 \leq z \leq 0.50$. They found major mergers contribute on average $48\% \pm 17\%$ toward the stellar mass of present day BGGs since $z = 0.32$. This corresponds to a stellar mass growth rate of $\sim 17\% \text{ Gyr}^{-1}$. These results are plotted as blue points in Figure 7. They find significantly higher stellar mass growth from major mergers than we do here.

Overall, we find that our results are in good agreement with the stellar mass growth calculated by McIntosh et al. (2008); Liu et al. (2009) and Robotham et al. (2014). However, the growth predicted by Liu et al. (2015) and Groenewald et al. (2017) is significantly larger. This is not unexpected due to the different methods employed by these studies. These growth rates were calculated with either purely photometric galaxy surveys (e.g., McIntosh et al. 2008; Liu et al. 2009; Edwards & Patton 2012; Liu et al. 2015) or incomplete spectroscopic surveys (e.g., Groenewald et al. 2017). McIntosh et al. (2008) and Liu et al. (2009) refined their search for close-companion galaxies by visually inspecting their sample of BGGs for signs of merging. This ensures that the galaxies selected are true close-companion galaxies such that their growth rates are consistent with our robust measurements from a highly complete spectroscopic survey. The stellar mass growth rates estimated by Edwards & Patton (2012), Liu et al. (2015) and Groenewald et al. (2017) are larger suggesting that the corrections applied for close-companion galaxies are not conservative enough.

5.3.2. Observational Studies of Change in Stellar Mass

Other studies such as Lidman et al. (2012) and Oliva-Altamirano et al. (2014) estimate the stellar mass growth of BGGs via a direct examination of the change in stellar mass of BGGs from higher to lower redshifts. Lidman et al. (2012) find that the stellar mass of BGGs increases by a factor of 1.8 ± 0.3 between $z \sim 0.9$ and $z \sim 0.2$, approximately equivalent to 5 Gyr.

Oliva-Altamirano et al. (2014) also directly examined the change in stellar mass of BGGs at low and high redshifts, $0.09 \leq z \leq 0.27$, using a large sample of 883 galaxies from an earlier release of the GAMA survey. They found an average stellar mass growth from $z = 0.27$ to $z = 0.09$ of $-7\% \pm 9\%$. This suggests that BGGs do not grow significantly over this redshift range. Our result agrees that BGGs do not grow in stellar mass significantly at low redshifts. It is important to note that while these results are drawn from the same survey, the stellar mass growth of the BGGs are estimated with independent methods.

5.3.3. Stellar Mass Growth in Models

Semianalytical models (e.g., De Lucia & Blaizot 2007; Laporte et al. 2013; Contini et al. 2014) used the Millennium Simulation (Springel et al. 2005) to study the formation and evolution of BGGs. The results of these models are largely similar. Both De Lucia & Blaizot (2007) and Laporte et al. (2013) find that BGGs grow by a factor of ~ 1.8 at low redshifts ($z < 0.5$), which is similar to that found observationally by Lidman et al. (2012). This is equivalent to a growth in stellar mass of $\sim 15\%$ per gigayear, which is significantly larger than what we find observationally. However, further evolution of the model in De Lucia & Blaizot (2007) explored in Contini et al. (2014), which accounts for the parallel growth of the intracluster light from massive merging galaxies, finds that the intracluster light fraction in groups and clusters ranges between 20% and 40%. Central galaxies in this updated model do not grow significantly at low redshifts, having a mass of approximately 97% of their total mass at $z \sim 0.2$. This agrees with the results obtained here.

6. Conclusion

In this paper, we have examined the potential for stellar mass buildup of BGGs in the local universe due to major mergers. We have analyzed a large volume-limited sample of 550 groups with spectroscopic redshifts between $0.07 \leq z < 0.2$ from the Galaxy And Mass Assembly (GAMA) survey (Liske et al. 2015). This data set is highly spectroscopically complete with a survey magnitude limit of $m_r > 19.8$ mag, which allows us to robustly analyze the impact of merging companion galaxies.

We selected a volume-limited sample of groups identified within the GAMA Galaxy Group Catalogue (Robotham et al. 2011). The BGGs studied here lie at the center of these groups and possess stellar masses between $10^{11.0} M_{\odot}$ and $10^{11.6} M_{\odot}$, where the stellar masses are sourced from the GAMA Stellar Mass catalog (Taylor et al. 2011).

We identified close-companion galaxies within a projected radius of 30 kpc of the central BGG with relative velocities $\Delta \leq 300 \text{ km s}^{-1}$ as a proxy to estimate the potential for stellar mass growth of BGGs within our sample. We investigated potential major merger candidates with mass ratios $M_{\text{BGG}}/M_{\text{CC}} \leq 4$.

Within our sample of 550 groups, we identified 17 close-companion galaxies. This resulted in a total pair fraction of 0.03 ± 0.01 with no significant evolution over the redshift range studied here. We also investigated the dependence on halo mass and, while we found no statistically significant dependence, we do observe a systematic decrease in the BGG pair fraction with increasing halo mass.

The close-companion galaxies in our sample will merge with their respective BGGs in $T_{\text{merge}} = 0.53 \pm 0.19$ Gyr, estimated using the merging timescale derived in Kitzbichler & White (2008). This combined with the pair fraction resulted in an average merger rate of $0.06 \pm 0.03 \text{ Gyr}^{-1}$ for BGGs in our sample. This results in a potential average stellar mass growth of $2.19\% \pm 1.52\% \text{ Gyr}^{-1}$ over $0.07 < z < 0.2$ due to major mergers. This is in good agreement with other observational studies that investigate the stellar mass buildup of BGGs via mergers; however, it is lower than that predicted by semianalytical models.

In a future analysis, we will use recent cosmological simulations such as ILLUSTRIS, EAGLE, and SIMBA (Vogelsberger et al. 2014; Schaye et al. 2015; Davé et al. 2019, respectively) to directly compare with these observational results to further validate the use of close-companion galaxies as a proxy for BGG stellar mass growth.

The authors thank the anonymous referee for their comments which improved the paper.








GAMA is a joint European-Australasian project based around a spectroscopic campaign using the Anglo-Australian Telescope. The GAMA input catalog is based on data taken from the Sloan Digital Sky Survey and the UKIRT Infrared Deep Sky Survey. Complementary imaging of the GAMA regions is being obtained by a number of independent survey programmes including GALEX MIS, VST KiDS, VISTA VIKING, WISE, Herschel-ATLAS, GMRT and ASKAP providing UV to radio coverage. GAMA is funded by the STFC (UK), the ARC (Australia), the AAO, and the participating institutions. The GAMA website is <http://www.gama-survey.org/>.

The authors acknowledge the Traditional Custodians and the Elders past and present of the land in which the Anglo-Australian Telescope stands, the Gamilaraay people, and the Bedegal people who are the Traditional Custodians of the land, of which much of this research was conducted, at UNSW Sydney.

The authors would like to thank C. Conselice for his invaluable comments during the preparation of this paper.

S.B. acknowledges funding support from the Australian Research Council through a Future Fellowship (FT140101166). A.R. acknowledges funding support from the Australian Research Council through a Future Fellowship (FT200100375).

ORCID iDs

K. Banks  <https://orcid.org/0000-0001-5210-1696>
 S. Brough  <https://orcid.org/0000-0002-9796-1363>
 B. W. Holwerda  <https://orcid.org/0000-0002-4884-6756>
 A. M. Hopkins  <https://orcid.org/0000-0002-6097-2747>
 Á. R. López-Sánchez  <https://orcid.org/0000-0001-8083-8046>
 K. A. Pimbblet  <https://orcid.org/0000-0002-3963-3919>
 A. S. G. Robotham  <https://orcid.org/0000-0003-0429-3579>

References

- Beers, T. C., Flynn, K., & Gebhardt, K. 1990, *AJ*, 100, 32
 Bellstedt, S., Lidman, C., Muzzin, A., et al. 2016, *MNRAS*, 460, 2862
 Brough, S., Couch, W. J., Collins, C. A., et al. 2008, *MNRAS*, 385, L103
 Cameron, E. 2011, *PASA*, 28, 128
 Casteels, K. R. V., Conselice, C. J., Bamford, S. P., et al. 2014, *MNRAS*, 445, 1157
 Cerulo, P., Orellana, G. A., & Covone, G. 2019, *MNRAS*, 487, 3759
 Collins, C. A., Stott, J. P., Hilton, M., et al. 2009, *Natur*, 458, 603
 Conroy, C., Wechsler, R. H., & Kravtsov, A. V. 2007, *ApJ*, 668, 826
 Contini, E., De Lucia, G., Villalobos, Á., & Borgani, S. 2014, *MNRAS*, 437, 3787
 Cooke, K. C., Kartaltepe, J. S., Tyler, K. D., et al. 2019, *ApJ*, 881, 150
 Davé, R., Anglés-Alcázar, D., Narayanan, D., et al. 2019, *MNRAS*, 486, 2827
 De Lucia, G., & Blaizot, J. 2007, *MNRAS*, 375, 2
 Driver, S. P., Hill, D. T., Kelvin, L. S., et al. 2011, *MNRAS*, 413, 971
 Duncan, K., Conselice, C. J., Mundy, C., et al. 2019, *ApJ*, 876, 110
 Edwards, L. O. V., & Patton, D. R. 2012, *MNRAS*, 425, 287
 Fraser-McKelvie, A., Brown, M. J. I., & Pimbblet, K. A. 2014, *MNRAS*, 444, L63
 Gozaliasl, G., Finoguenov, A., Khosroshahi, H. G., et al. 2016, *MNRAS*, 458, 2762
 Groenewald, D. N., Skelton, R. E., Gilbank, D. G., & Loubser, S. I. 2017, *MNRAS*, 467, 4101
 Gunn, J. E., Gott, J., & Richard, I. 1972, *ApJ*, 176, 1
 Hansen, S. M., Sheldon, E. S., Wechsler, R. H., & Koester, B. P. 2009, *ApJ*, 699, 1333
 Hill, D. T., Kelvin, L. S., Driver, S. P., et al. 2011, *MNRAS*, 412, 765
 Hopkins, A. M., Driver, S. P., Brough, S., et al. 2013, *MNRAS*, 430, 2047
 Hopkins, P. F., Croton, D., Bundy, K., et al. 2010, *ApJ*, 724, 915
 Kelvin, L. S., Driver, S. P., Robotham, A. S. G., et al. 2012, *MNRAS*, 421, 1007
 Kitzbichler, M. G., & White, S. D. M. 2008, *MNRAS*, 391, 1489
 Kravtsov, A. V., Vikhlinin, A. A., & Meshcheryakov, A. V. 2018, *AsL*, 44, 8
 Laporte, C. F. P., White, S. D. M., Naab, T., & Gao, L. 2013, *MNRAS*, 435, 901
 Lavoie, S., Willis, J. P., Démoclès, J., et al. 2016, *MNRAS*, 462, 4141
 Lidman, C., Suherli, J., Muzzin, A., et al. 2012, *MNRAS*, 427, 550
 Lidman, C., Iacobuta, G., Bauer, A. E., et al. 2013, *MNRAS*, 433, 825
 Lin, Y.-T., Brodwin, M., Gonzalez, A. H., et al. 2013, *ApJ*, 771, 61
 Lin, Y.-T., & Mohr, J. J. 2004, *ApJ*, 617, 879
 Liske, J., Baldry, I. K., Driver, S. P., et al. 2015, *MNRAS*, 452, 2087
 Liu, F. S., Lei, F. J., Meng, X. M., & Jiang, D. F. 2015, *MNRAS*, 447, 1491
 Liu, F. S., Mao, S., Deng, Z. G., Xia, X. Y., & Wen, Z. L. 2009, *MNRAS*, 396, 2003
 Liu, F. S., Mao, S., & Meng, X. M. 2012, *MNRAS*, 423, 422
 Lotz, J. M., Jonsson, P., Cox, T. J., et al. 2011, *ApJ*, 742, 103
 Lotz, J. M., Jonsson, P., Cox, T. J., & Primack, J. R. 2008, *MNRAS*, 391, 1137
 McIntosh, D. H., Guo, Y., Hertzberg, J., et al. 2008, *MNRAS*, 388, 1537
 Miller, C. J., Nichol, R. C., Reichart, D., et al. 2005, *AJ*, 130, 968
 Mundy, C. J., Conselice, C. J., Duncan, K. J., et al. 2017, *MNRAS*, 470, 3507
 Murante, G., Giovalli, M., Gerhard, O., et al. 2007, *MNRAS*, 377, 2
 O’Dea, K. P., Baum, S. A., Privon, G., et al. 2008, *ApJ*, 681, 1035
 O’Dea, K. P., Quillen, A. C., O’Dea, C. P., et al. 2010, *ApJ*, 719, 1619
 Oliva-Altamirano, P., Brough, S., Lidman, C., et al. 2014, *MNRAS*, 440, 762
 Popesso, P., Biviano, A., Böhringer, H., & Romaniello, M. 2007, *A&A*, 464, 451
 Puchwein, E., Springel, V., Sijacki, D., & Dolag, K. 2010, *MNRAS*, 406, 936
 Robotham, A., Driver, S. P., Norberg, P., et al. 2010, *PASA*, 27, 76
 Robotham, A. S. G., Norberg, P., Driver, S. P., et al. 2011, *MNRAS*, 416, 2640
 Robotham, A. S. G., Driver, S. P., Davies, L. J. M., et al. 2014, *MNRAS*, 444, 3986
 Rykoff, E. S., Rozo, E., Busha, M. T., et al. 2014, *ApJ*, 785, 104
 Schaye, J., Crain, R. A., Bower, R. G., et al. 2015, *MNRAS*, 446, 521
 Schombert, J. M. 1987, *ApJS*, 64, 643
 Springel, V., White, S. D. M., Jenkins, A., et al. 2005, *Natur*, 435, 629
 Taylor, E. N., Hopkins, A. M., Baldry, I. K., et al. 2011, *MNRAS*, 418, 1587
 Ventou, E., Contini, T., Bouché, N., et al. 2019, *A&A*, 631, A87
 Viola, M., Cacciato, M., Brouwer, M., et al. 2015, *MNRAS*, 452, 3529
 Vogelsberger, M., Genel, S., Springel, V., et al. 2014, *MNRAS*, 444, 1518
 Webb, T. M. A., Muzzin, A., Noble, A., et al. 2015, *ApJ*, 814, 96
 York, D. G., Adelman, J., Anderson, J. E., et al. 2000, *AJ*, 120, 1579
 Zhao, D., Aragón-Salamanca, A., & Conselice, C. J. 2015, *MNRAS*, 453, 4444
 Zhao, D., Conselice, C. J., Aragón-Salamanca, A., et al. 2017, *MNRAS*, 464, 1393